# How to Build a Model of the Atmosphere and Spectrum

Robert L. Kurucz

**Abstract** We want to include the opacity of millions or hundreds of millions of lines in model stellar atmosphere calculations, then generate detailed, realistic spectra from those model atmospheres, then model the observation process, and finally compare the calculated spectra to observed spectra to determine the properties of stars so that we can understand their evolution and the evolution of galaxies.

## 1 Introduction

Building an LTE, hydrostatic equilibrium model starts by specifying $T_{eff}$, log g, and abundances. Then you guess a temperature-optical depth relation (using a starting model) for many layers in the photosphere. Then you iterate through the following steps until the flux is constant and temperature is stationary at each layer in the atmosphere.

Compute the equation of state to determine the population of each species and the pressure in each layer.
Compute the line and continuum opacity.
Compute the radiation field and the total radiative flux in each layer.
Compute the convective flux in each layer.
Compute the total flux error and the correct the temperature in each layer.

All of this was described in SAO Special Report 309 more than 40 years ago. Some of the coding has not changed since before SR 309 was written about ATLAS5. Current versions of ATLAS are much more sophisticated. The report is on

Robert L. Kurucz
Harvard-Smithsonian Center for Astrophysics, 60 Garden Street, Cambridge, MA 02138, USA
e-mail: rkurucz@cfa.harvard.edu

my website **kurucz.harvard.edu/papers** as are the previous series of talks I gave in Trieste in 2005:

/SAO309 ATLAS: A computer program for calculating model stellar atmospheres. SAO Special Report No. 309, 1970.

/TRIESTEATLAS12 ATLAS12, SYNTHE, ATLAS9, WIDTH9, etc. (Kurucz 2005a)

/TRIESTELIMITS Physical, numerical, and computational limits for Kurucz codes. (Kurucz 2005b)

/TRIESTERAPID Rapid computation of line opacity in SYNTHE and DFSYNTHE. (Kurucz 2005c)

/TRIESTELINES Including all the lines. (Kurucz 2005d)

/TRIESTESOLAR New atlases for solar flux, irradiance, central intensity, and limb intensity. (Kurucz 2005e)

Here I will discuss details of topics that are not in textbooks but that affect the accuracy of the results you are able to obtain: observational and computational pipelines; rotation; equation of state; convection and microturbulent velocity.

In my next lecture I will talk about three treatments of opacity and the corresponding programs: Resolved spectra and SYNTHE; Sampled spectra and ATLAS12; Low resolution distribution functions and DFSYNTHE and ATLAS9.

## 2 Observational and Computational Pipelines

Radiation from a star is affected by a series of interactions before it appears on your terminal screen as a spectrum. These are outlined in the observational pipeline column in Fig. 1. Each interaction can be modelled computationally, although, in practice, some are treated empirically and some are ignored.

| Observational Pipeline | Computatonal Pipeline | Programs |
|---|---|---|
| | Grid of models and | ATLAS9/12+ |
| Rotating star | intensity spectra | SYNTHE |
| | Interp. rotated flux spectrum | ROTATE |
| Circumstellar material | Circumstellar transmission | not yet |
| ISM reddening | ISM reddening | REDDEN |
| ISM lines | ISM lines | not yet |
| ISM diffuse bands | ISM diffuse bands | not yet |
| Telluric airglow | Telluric airglow | not yet |
| Anthropogenic light | Anthropogenic light | not yet |
| Telluric broad features | Telluric broad features | TRANSYNTHE |
| Telluric lines | Telluric lines | TRANSYNTHE |
| Aerosols | Aerosols | not yet |
| Telescope transmission | From reduction procedure | |
| Instrumental transmission | From reduction procedure | |
| Scattered light | From reduction procedure | |
| Detector sensitivity | From reduction procedure | |
| Cosmic rays+radioactivity | Removed by red. procedure | |
| Instrumental profile | From reduction procedure | BROADEN |
| Observed spectrum | Computed spectrum | |
| Compare to observed spectrum | | PLOTSYN |
| Iterate | | |

**Fig. 1** Observational and computational pipelines.

## 3 Rotation

All stars rotate. Except for a tiny percentage that are observed exactly pole-on, the rotation broadens the lines in the spectrum. Observationally the star sends a ray of intensity spectrum toward us from each point on the disk and it Doppler shifts that spectrum by the projected rotation velocity at that point. The total flux spectrum directed at us is the integral over all the rays.

For a slowly rotating, spherical star, computing the flux spectrum is a straightforward process. In ROTATE I tabulate intensity spectra as a function of angle from disk center (limb darkened spectra). I put a grid over the disk, say $200\times200$ or $400\times400$ points, and determine the angle and Doppler shift at each point. (Symmetries are taken into account.) I interpolate to each grid point, Doppler shift the spectrum, and add it to the integrand for the rotated flux spectrum.

One complication is that if you look at the sun with high quality spectra you can actually see differential rotation in the line profiles. Presumably, rapidly rotating stars have strong differential rotation as well. I have put in an option in ROTATE to compute differential rotational broadening.

The spherical assumption is fine for old, tired stars but young stars are fast rotators, and early type stars can be so fast that they are oblate and have gravity darkening. Fig. 2 shows the observed structure of Altair from interferometry by Peterson et al. (2006). Fig. 3 shows Vega determined by Yoon et al. (2010). Vega looks almost spherical because it is observed almost pole-on. Until recently spectra and the SED (spectral energy distribution) were not determined well enough to show the oblateness and gravity-darkening. The star could be well matched with a simple plane-parallel model, Figs. 4 and 5 (Kurucz 1979). This shows that you can get away with an awful lot if you stick to low resolution.

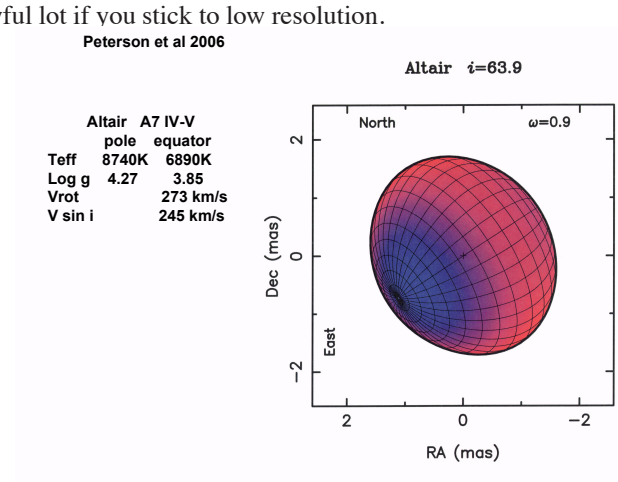


**Fig. 2** Altair projected against the sky with derived parameters.

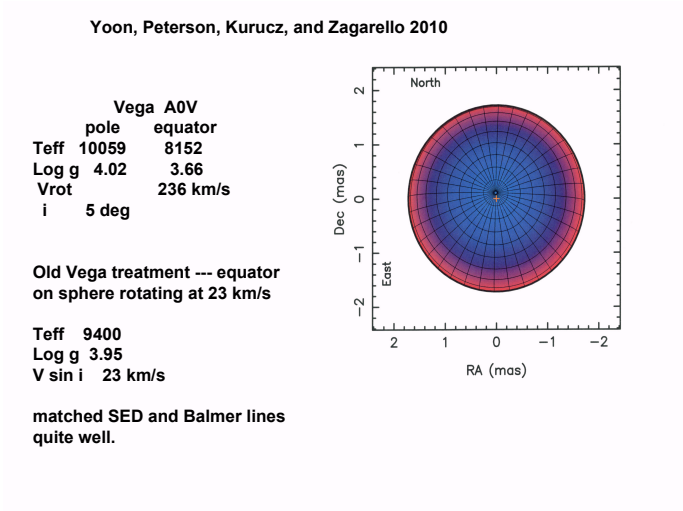


**Fig. 3** Vega projected against the sky with derived parameters.

If we (Yoon et al. 2010) assume that we understand gravity darkening, these stars can be straighforwardly modelled (but we probably do not.) As before we place a grid over the star. At each point we determine the angle, the velocity, $T_{eff}$, and log g. We compute a grid of models and spectra covering the whole range of $T_{eff}$ and log g that are possible on the surface. For each model we compute the intensity spectrum as a function of angle. Then we interpolate the spectrum in $T_{eff}$, log g, angle, and Doppler shift at each point and add it to the integrand for the rotated flux spectrum. (I am not yet distributing this version of ROTATE).

## 4 Circumstellar and Interstellar Absorption

Continuing through the pipeline, Fig. 1:

Circumstellar gas and dust from mass loss, thick disks, zodiacal disks can absorb and produce spectral features and modify the SED.

Interstellar reddening. Program REDDEN reddens SEDs with simple models.

Interstellar diffuse bands. Herbig (1995) has a catalogue of bands.

Interstellar lines. Just search through my line lists for strong lines with lower energies less than 300 $cm^{-1}$.

These programs are not yet written. Any of you could do it. At present be aware of interstellar features and avoid them.

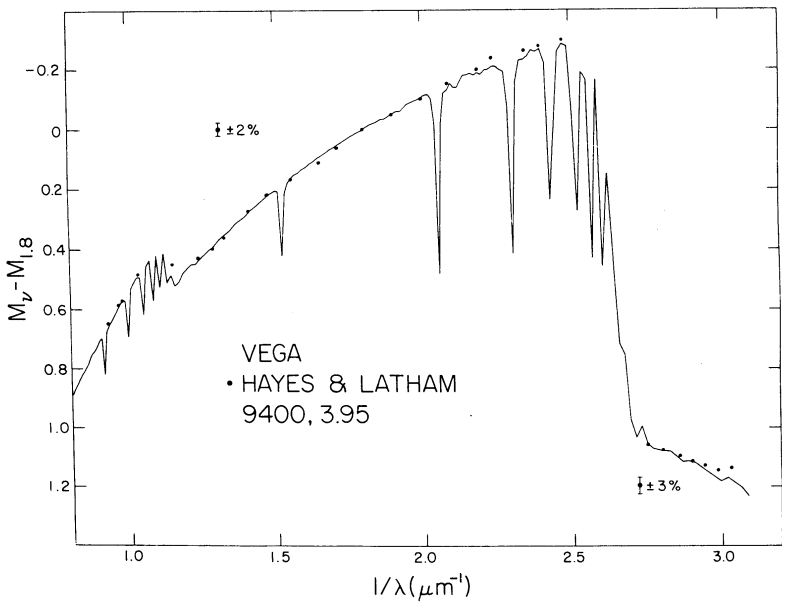


**Fig. 4** Old fit to Vega SED from Hayes and Latham (1975) (Kurucz 1979).

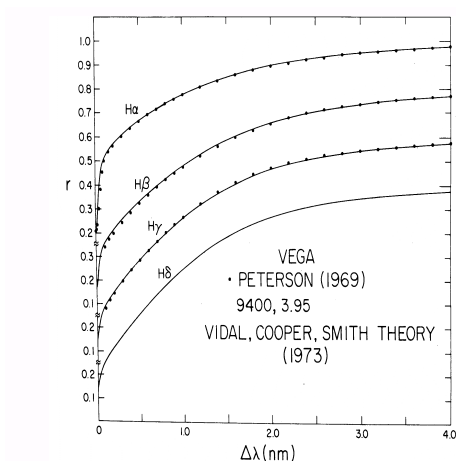


**Fig. 5** Old fit to Vega Balmer profiles measured by Peterson (1969) (Kurucz 1979).

## 5 Telluric Spectra

Continuing through the earth's atmosphere:

Telluric airglow. $O_2$, OH, NO, and other radicals at altitudes above 70 km add emission lines to the spectrum. There are atlases and line catalogues by Osterbrock et al. (2000) and by Cosby et al. (2006), for example. I have not yet programmed it.

Anthropogenic light. There are many city lights in southern Arizona and at other sites that add emission lines to the spectrum. There is a line catalogue by Slanger et al. (2003). I have not yet programmed it.

Any of you could write these programs. In the meantime be aware of the possibility of emission lines.

I have written programs for atmospheric transmission. Given an atmospheric model, which is like a stellar model, temperature and pressure as a function of altitude, program TRANSYNTHE computes the opacity. Then program TRANSPECTR computes the mean transmission from beginning to end of an observation through the atmosphsere down to the telescope.

Fig. 6 shows absorption by ozone $O_3$ and $O_2$ dimer $[O_2]_2$. Fig. 7 shows absorption by $O_2$ and $H_2O$ lines in the visible. Including telluric lines requires very high resolution. I typically use a resolving power of 2 million. That same resolution is then required in computing the stellar spectrum because the spectra are multiplied together point by point by program TRANSMIT. Most of the line data come from the HITRAN line list by Rothman et al. 2005, formerly US Air Force, now Smithsonian Astrophysical Observatory. There is a new edition at **www.cfa.harvard.edu/hitran**. I reformat the HITRAN data into Kurucz format so they can be used as stellar opacity as well.

I have not yet programmed aerosols. They are not significant for residual spectra but matter for absolute spectrophotometry.

## 6 Comparison to Observed Spectra

Program BROADEN runs the computed spectrum through the measured instrumental profiles. The profile can range from a simple Gaussian to a complicated asymmetric shape with wing structure. (At this stage you can generate spectra at any lower resolution as well, even down to resolving power 100.)

Then I plot the observed and computed spectra on top of each other with the lines labelled using program PLOTSYN to identify the features and to see what is wrong and what is right. Fig. 8 is a Space Telescope spectrum of Sirius at 201 nm. I like it because it illustrates a number of problems.

The observed structures in black are not lines but features that are blends of lines. The 16 km/s rotation blends the lines together. I have also plotted the spectrum computed with no rotation in blue. This helps indicate the composition of blends.

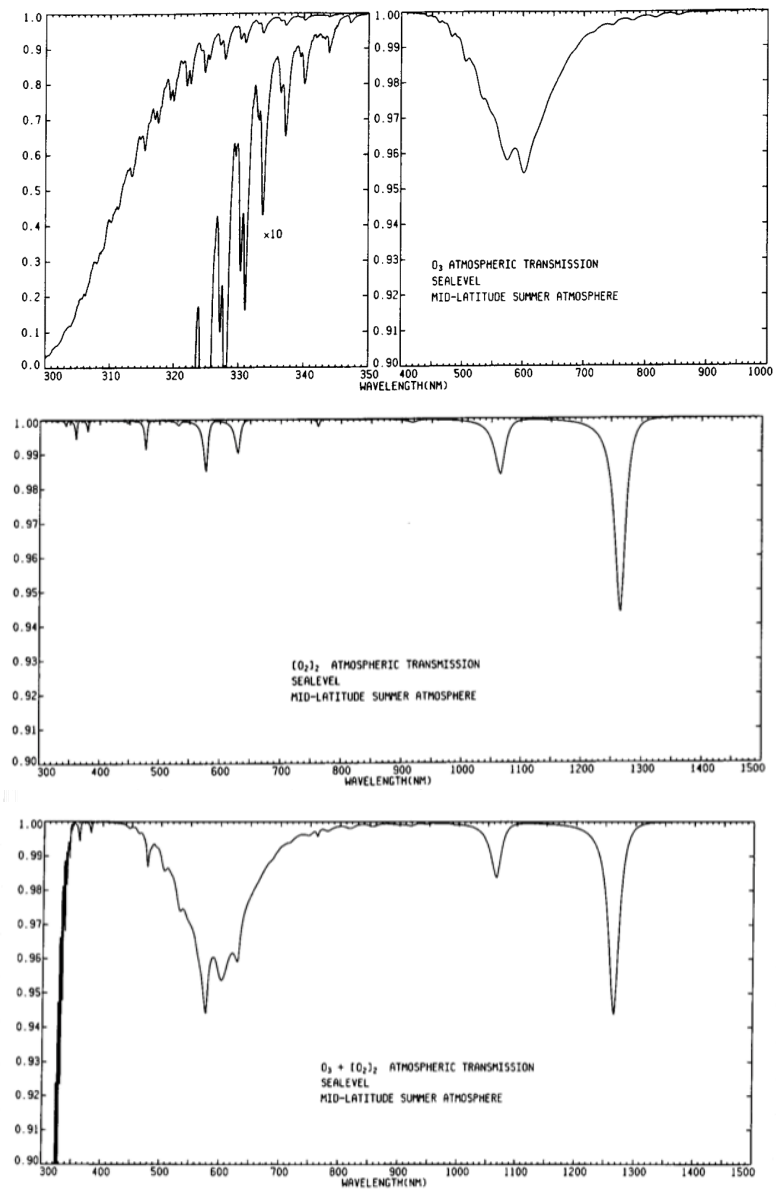


**Fig. 6** Atmospheric absorption by ozone and $O_2$ dimer

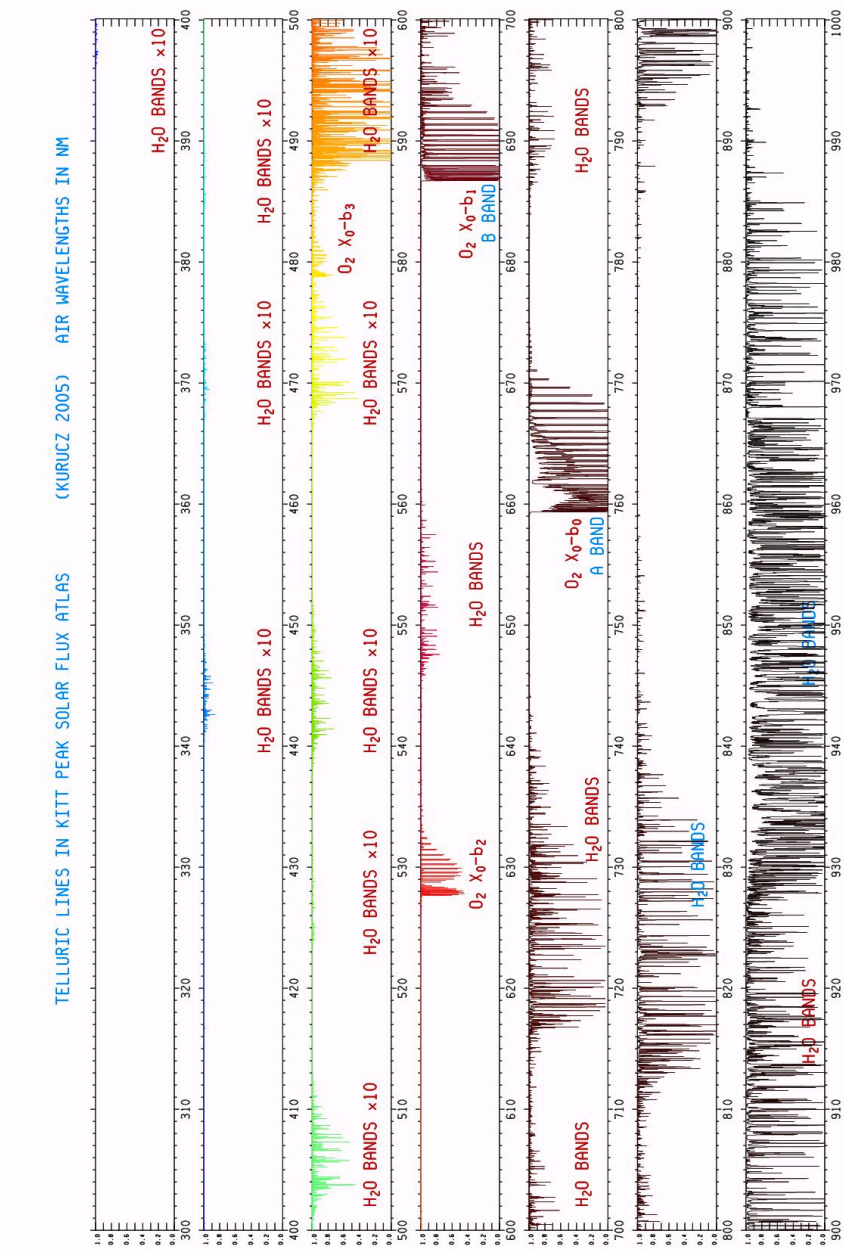


**Fig. 7** Telluric lines in Kitt Peak Solar Flux Atlas (Kurucz 2005).

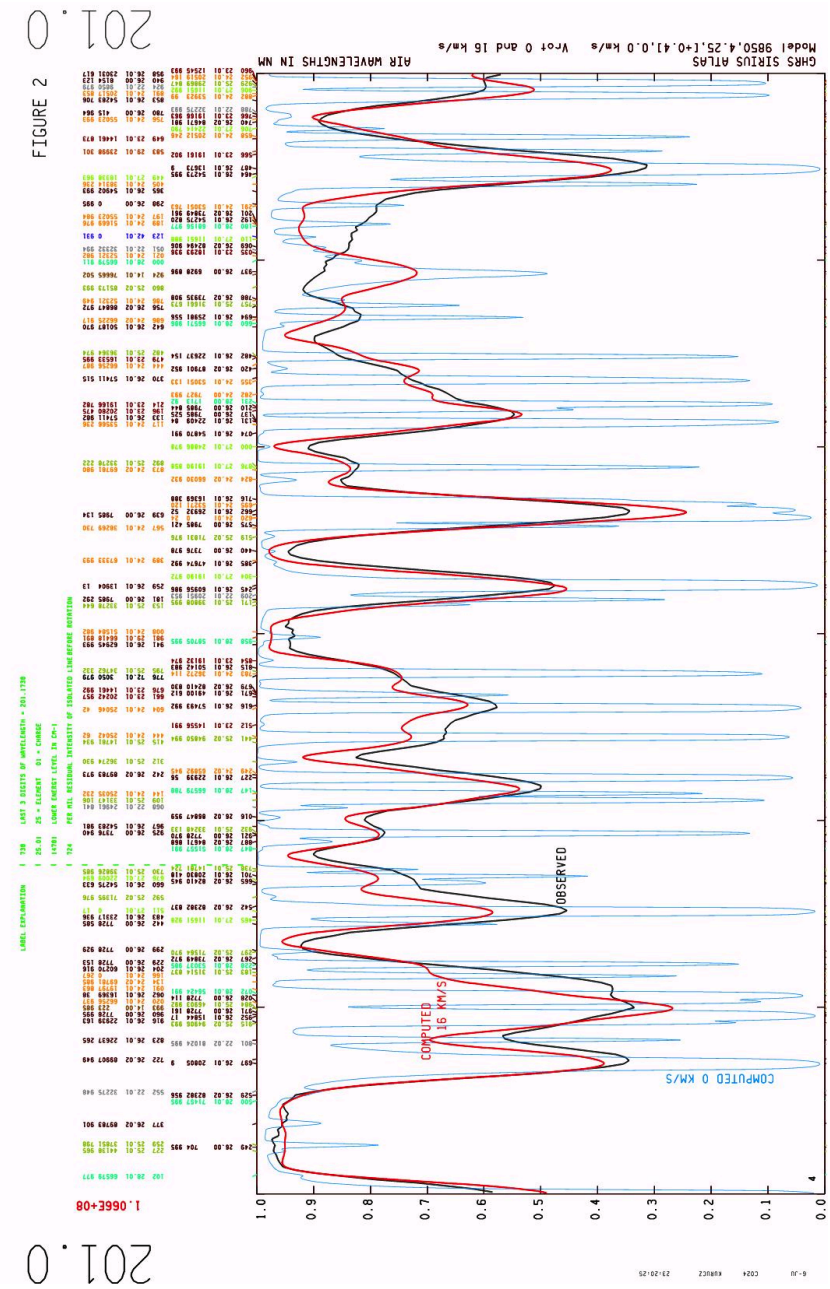


**Fig. 8** Comparison of computed and observed Space Telescope GHRS spectra of Sirius.

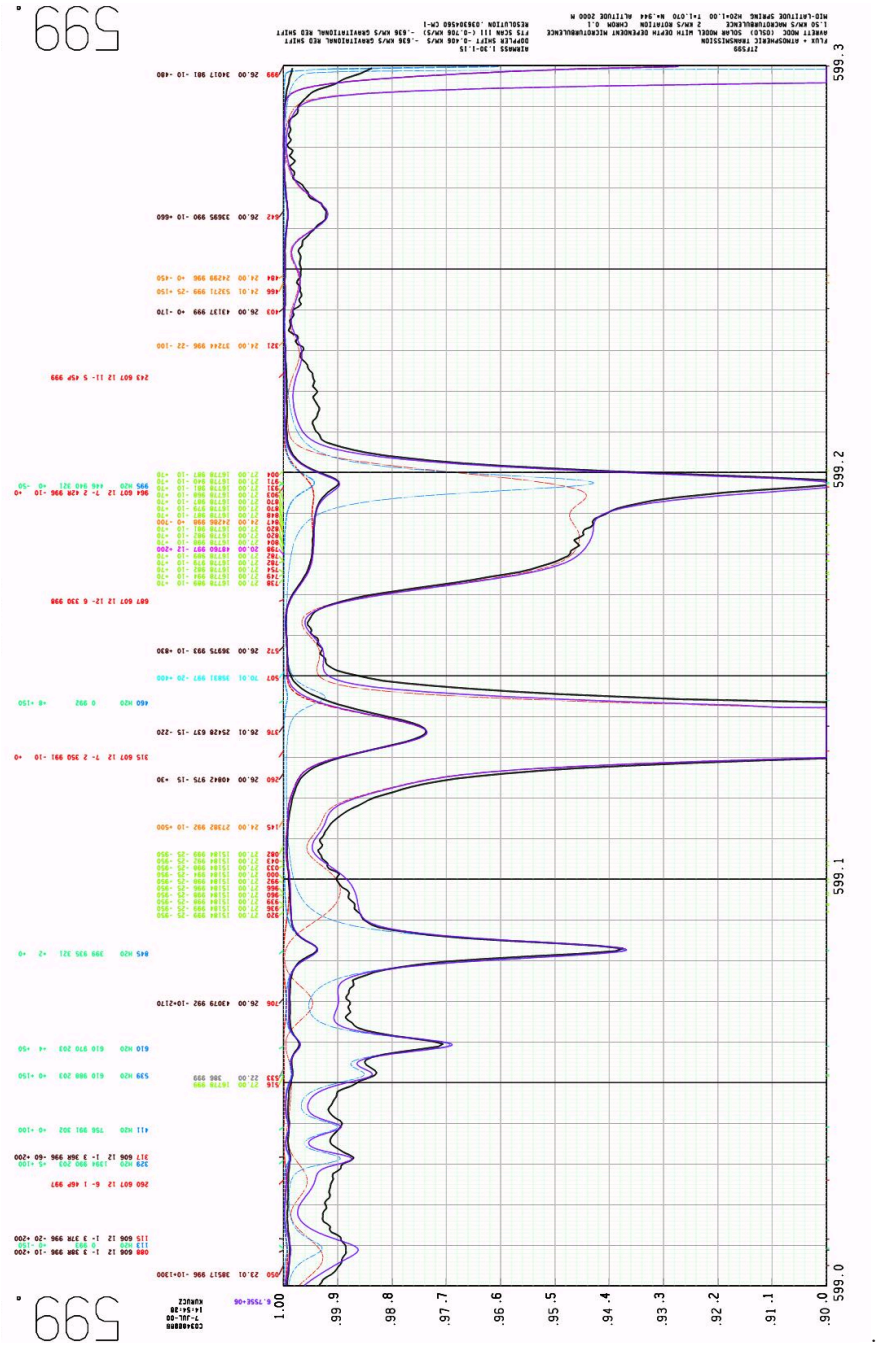


**Fig. 9** Comparison of computed and observed Kitt Peak FTS solar spectra.

The minima of the features are not line positions. They frequently fall in between two lines as at 201.1 nm and 201.41 nm. They cannot be used to set or check a wavelength scale.

Some lines are too weak, (201.14 nm); or missing, (201.11 nm); or too strong, (201.49 nm).

Fig. 9 shows a section of solar spectrum at 599 nm where each spectrum is plotted twice, once at normal scale and once at 10 times scale to show small differences. The observed spectrum is black, the computed solar spectrum is red, the telluric spectrum is blue, and the transmitted spectrum is magenta.

## 7 Equation of State

All physical data change, hopefully for the better, as time goes by. Even the speed of light has been revised over the lifetime of these programs but is now fixed. Laboratory analyses of atoms and molecules have improved tremendously. There are much more accurate energies and with many more levels known. There are many more lines and with better wavelengths. Partition functions, ionization potentials, and equilibrium constants have changed. I am computing new partition functions and equilibrium constants as I compute new line lists to update the equation of state sections of my programs. You should be aware that the data for ions or molecules that have not been updated can be 30 or 40 years out of date.

## 8 Convection and Microturbulent Velocity

Fig. 10 is the empirical solar model C from Fontenla, Avrett, and Loeser 1993. The upper darker line is the temperature distribution which drops through the photosphere to the temperature minimum and then rises in the chromosphere. They also determined the microturbulent velocity which drops through the photosphere to a minimum and then rises in the chromosphere. The maximum microtubulent velocity in the photosphere is also the maximum mixing-length convective velocity in my solar model ASUN. I interpret the photospheric microturbulent velocity as convective motions that go to zero in the radial direction toward the surface (Kurucz 1996). Then waves and magnetic motions produce an outwardly increasing chromospheric microturbulent velocity.

I assume that the microturbulent velocity varies the same way in all convective models and I scale the solar profile by the ratio of the maximum convective velocity over a grid of models to the solar maximum convective velocity. The left panel in Fig. 11 shows the maximum convective velocity for a solar abundance grid running from 3500K to 8500K and in log g from 5.0 down to 0.0 . You can see that for a $T_{eff}$ = 3500K, log g = 5.0 M dwarf the maximum is about 0.25 km $s^{-1}$; for $T_{eff}$ = 6000K, log g = 4.5 it is about 2 km $s^{-1}$. You also see that there is a family of

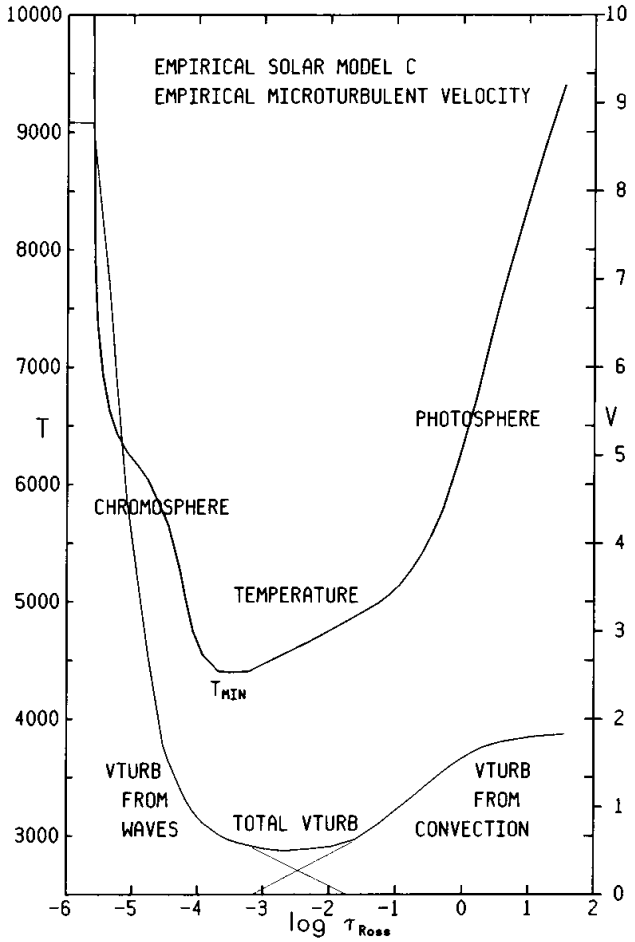


**Fig. 10** Empirical temperature and microturbulent velocity distributions in the sun (Fontenla, Avrett, and Loeser 1993).

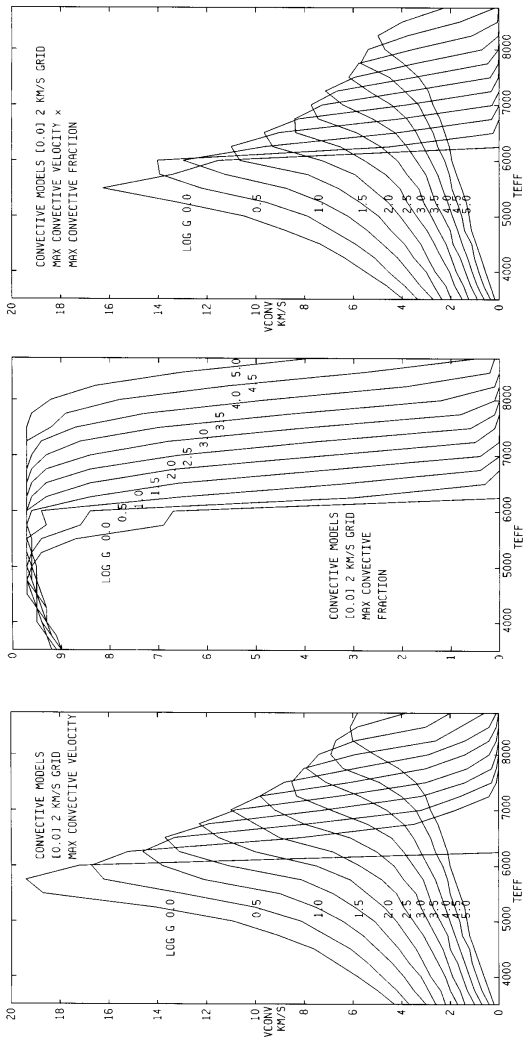


**Fig. 11** The maximum convective velocity in a solar abundance grid of models; the maximum convective fraction; the product.

smoothly increasing curves as the temperature increases until each curve reaches a maximum and the convection catastrophically falls off and disappears.

The center panel shows the maximum fraction of total flux carried by convection. In the right panel I weight the maximum convective velocities by this fraction and they are the numbers I use to scale the microturbulent velocity.

At the higher temperatures convective microturbulence decreases and disappears. The microturbulence may actually be zero or other kinds of "microturbulence" may take over. For example, pulsation produces differential velocities that broaden lines.

## References

1. P.C. Cosby, B.D. Sharpee, T.G. Slanger, D.L. Huestis, R.W. Hanuschik. J. Geophys. Res, 111, A12307, 14pp.
2. J.M. Fontenla, E.H. Avrett, and R. Loeser. Astrophys. J. **406**, 319–345 (1993)
3. D.S. Hayes and D.W. Latham. Astrophys. J. **197**, 593–601 (1975)
4. G.H. Herbig. Ann. Rev. Astron. Astrophys. **33**, 19–73 (1995)
5. R.L. Kurucz. Astrophys. J. Supp. **40**, 1–340 (1979)
6. R.L. Kurucz. Astron. Soc. Pacific Conf. Ser. **108** 2–18 (1996)
7. R.L. Kurucz. Mem. Soc. Astron. Ital. Suppl. **8**, 10–20 (2005a)
8. R.L. Kurucz. Mem. Soc. Astron. Ital. Suppl. **8**, 69–71 (2005b)
9. R.L. Kurucz. Mem. Soc. Astron. Ital. Suppl. **8**, 72–73 (2005c)
10. R.L. Kurucz. Mem. Soc. Astron. Ital. Suppl. **8**, 83–92 (2005d)
11. R.L. Kurucz. Mem. Soc. Astron. Ital. Suppl. **8**, 158–160 (2005e)
12. R.L. Kurucz. Kitt Peak Solar Flux Atlas (2005f). kurucz.harvard.edu/sun/fluxatlas2005
13. R.L. Kurucz. Kitt Peak Solar Irradiance Atlas (2005g). kurucz.harvard.edu/sun/irradiance2005
14. R.L. Kurucz. Irradiance in the H and K bands (2008). kurucz.harvard.edu/sun/irradiance2008
15. D.E. Osterbrock, R.T. Waters, T.A. Barlow, T.G. Slanger, P.D. Cosby. PASP **112**, 733-741 (2000)
16. D.M. Peterson. SAO Spec. Rep. No. 293, 199pp. (1969)
17. D.M. Peterson, C.A. Hummel, T.A. Pauls, et al. Astrophys. J. **636**, 1087–1097 (2006)
18. L.S. Rothman et al. JQSRT **96**, 139-204 (2005)
19. T.G. Slanger, P.C. Cosby, D.E. Osterbrock, R.P.S. Stone, and A.A. Misch. PASP **115**, 869–878 (2003)
20. C.R. Vidal, J. Cooper, E.W. Smith. Astroph. J. Supp. **25**, 37–136 (1973)
21. J. Yoon, D.M. Peterson, R.L. Kurucz, and R.J. Zagarello. Astrophys. J. **708**, 71–79 (2010)